ELSEVIER

Food Hydrocolloids 18 (2004) 1023–1031

FOOD HYDROCOLLOIDS

www.elsevier.com/locate/foodhyd

Time evolution of phase separating milk protein and amylopectin mixtures

Petra W. de Bont[a], Cris L. Luengo Hendriks[b], Geert M.P. van Kempen[a], Rob Vreeker[a,*]

[a]*Unilever Research and Development Vlaardingen, Olivier van Noortlaan 120, 3133 AT Vlaardingen, The Netherlands*
[b]*Delft University of Technology, Delft, The Netherlands*

Received 12 November 2003; revised 23 December 2003; accepted 2 April 2004

Abstract

The time evolution of phase separating milk protein–amylopectin mixtures at pH 6.3 was studied by confocal scanning laser microscopy (CSLM). CSLM measurements revealed the formation of aggregate-like structures of protein particles. Two different procedures, 2-D Fourier transformation and morphological sieving, were used to analyse the CSLM images. Both procedures showed the existence of a characteristic length scale (Λ) in the system, which evolved with time (t) according to a power law, $\Lambda \sim t^{\alpha}$. The power-law exponent α depended on the amylopectin concentration in the mixture. At relatively low concentrations $\alpha \cong 0.2$, which is compatible with theoretical predictions for 'late stage' coarsening. At relatively high amylopectin concentrations a much lower power of ca. 0.04 was observed, indicative of a very slow growth process. The slow growth may be explained from earlier work [Food Hydrocolloids 16 (2002) 127], which showed that at sufficiently high amylopectin concentrations a protein particle network develops with gel-like properties. The morphological sieving method in addition yielded information on the size of the protein-rich and amylopectin-rich domains in the CSLM images.

Keywords: Phase separation; Microstructure; Evolution; Confocal microscopy; Fourier Transform; Morphological Sieving

1. Introduction

Polysaccharides are often used as thickening agents or stabilisers in dairy-based products. Their main functions are to improve product texture (organoleptic properties) and physical stability (water binding). Mixtures of proteins and polysaccharides are often unstable. After preparation they tend to demix into protein-rich areas and polysaccharide-rich areas. This phenomenon is called phase separation. Several authors have recently studied phase separation in milk protein (colloidal casein) and polysaccharide mixtures. Schorsch, Clark, Jones, and Norton (1999), Schorsch, Jones, and Norton (1999), and Bourriot, Garnier, and Doublier (1999a,b,c) measured phase diagrams for micellar casein–locust bean gum, guar gum and κ-carrageenan mixtures. Tuinier and de Kruif (1998, 1999) studied phase separation in mixtures of milk protein and exocellular polysaccharide produced by a lactic acid bacterium. In this last case the observed phase behaviour was analysed on the basis of Vrij's depletion theory for colloid–polymer mixtures (Vrij, 1976). Milk was considered as a dispersion of colloidal particles (casein micelles) with a radius $r_c \approx 100$ nm in an aqueous phase containing various minerals (calcium, magnesium, etc.), lactose and small (<5 nm) globular proteins. In the analysis, the casein micelles were considered to behave effectively as hard spheres (de Kruif, 1992). Exocellular polysaccharides added to the colloidal dispersion were assumed to cause attractive interactions between the casein particles as a result of depletion effects. The phase boundary between stable and unstable protein–polysaccharide mixtures was calculated and shown to be in good agreement with the experimentally observed phase boundary. This supports the idea that depletion interactions are the driving force for phase separation in these micellar milk protein–polysaccharide mixtures.

In our former study (de Bont, van Kempen, & Vreeker, 2002) we showed that Vrij's depletion theory for polymer and colloid mixtures could also account for phase separation in the case of milk protein–amylopectin mixtures. Confocal scanning laser microscopy (CSLM) revealed the appearance of protein aggregate structures in these systems. At relatively high amylopectin concentrations the protein aggregates form a network with gel-like properties.

* Corresponding author. Address: P.O. Box 114, 3130 AC Vlaardingen, The Netherlands. Tel.: +31-10-460-6505; fax: +31-10-460-5236.
E-mail address: rob.vreeker@unilever.com (R. Vreeker).

0268-005X/$ - see front matter © 2004 Elsevier Ltd. All rights reserved.
doi:10.1016/j.foodhyd.2004.04.007

This was supported by evidence obtained from small deformation rheology. The occurrence of aggregated structures was different from the emulsion-like microstructures, with milk proteins dispersed in spherical droplets, as observed e.g. in mixtures of milk protein–guar gum (de Bont et al., 2002) or milk protein–locust bean gum (Schorsch et al., 1999). The observed microstructural difference was tentatively explained using earlier experimental observations reported by Sperry (1984) and a theoretical description developed by Lekkerkerker, Poon, Pusey, Stroobants, and Warren (1992) and is ascribed to a low value of the polymer–colloid size ratio for milk protein–amylopectin systems.

The present study focuses on the kinetic aspects of phase separation in milk protein–amylopectin systems at pH 6.3. The development and growth of 'inhomogeneities' in the phase separating mixtures was followed as a function of time using CSLM. 2-D Fourier transform and morphological sieving were used as image analysis tools. Both procedures revealed the existence of a characteristic length scale (Λ) in the system, which evolved with time (t) according to a power law, $\Lambda \sim t^{\alpha}$. The obtained time-dependent growth curves were interpreted on basis of power-law theories for late-stage coarsening. Application of the sieving method made it possible to determine the sizes of the colloid (protein)-rich and polymer (amylopectin)-rich areas independently.

2. Kinetics of phase separation

Two different mechanisms of phase separation are generally distinguished: the nucleation and growth (NG) mechanism and the spinodal decomposition (SD) mechanism. NG is expected when the phase separating mixture is located in the metastable region of the phase diagram (i.e. between the binodal and spinodal curves). In this region the system is stable to small concentration fluctuations. Small fluctuations decay unless they exceed a certain critical size. Once a nucleus of critical size is formed it remains stable and starts to grow. SD is expected for mixtures further away from the binodal (i.e. when the spinodal is crossed). In this 'unstable' region of the phase diagram, concentration fluctuations will always lead to a lowering of free energy and mixtures will decompose spontaneously into separate phases. The kinetics of phase separation by SD are characterised by three different stages: the early, intermediate and late stage of growth. The early stage is described by the (linear) Cahn–Hilliard theory (Cahn, 1965; Cahn & Hilliard, 1958). The theory predicts that for any situation there will be a particular wave that will grow fastest giving rise to a characteristic length scale (Λ) in the structure. During the early stage of SD the composition of the separating phases changes, but the characteristic length scale remains constant. As time goes on (in the intermediate regime) non-linear growth terms cause the demixing domains to move to larger length scales. A theoretical discussion of SD in the intermediate stage is given by Dhont (1996). In the late stage of decomposition, coarsening of the microstructure occurs and the charactertistic length scale $\Lambda(t)$ is related to time by a power law: $\Lambda(t) \propto t^{\alpha}$.

Power-law time dependencies are expected for both the NG and the SD mechanism. Different values for the power-law exponent are predicted, depending on the mechanism of coarsening. When coarsening occurs via diffusive transport of components (Ostwald ripening) an exponent of $\alpha = 1/3$ is predicted (Lifshitz & Slyozov, 1961; Tokuyama & Kawasaki, 1984). Smaller exponents ($\alpha = 1/4$) have been predicted in a pre-asymptotic regime and in cases where the interfacial width is relatively large (Butler, 2002 and references mentioned therein). When coarsening occurs via droplet coalescence an exponent of 1/3 or smaller is predicted, depending on whether the separation between droplets is approximately similar to the droplet size or larger (Butler, 2002; Tanaka, 2000). When coarsening is accelerated by (surface-tension driven) hydrodynamic flow in the system an exponent of 1 is expected (Siggia, 1979). Very low values of the coarsening exponent are predicted for mixtures in which one of the components gels. When gelation occurs, elastic terms enter into the expression for the free energy of the system, which tend to oppose phase separation and severely reduces coarsening of the microstructure. Onuki and Puri (1999) derived a relation between the cross-link density in the gel (ν) and the coarsening exponent of the form $\alpha = 1/3 - A\nu$, where A is a numerical constant. For sufficiently large cross-link densities, very low coarsening exponents (<0.1) are predicted.

Power-law coarsening has been observed experimentally in various demixing biopolymer and colloid–polymer systems (Butler, 2002; Butler & Heppenstall-Butler, 2001; Lorén, Altskär, & Hermansson, 2001; Lorén, Langton, & Hermansson, 2002; Koenderink, Aarts, de Villeneuve, Philipse, Tuinier, & Lekkerkerker, 2003; Rouw, Woutersen, Ackerson, & de Kruif, 1989; Tromp, Rennie, & Jones, 1995; Tuinier, Dhont, & de Kruif, 2000; Verhaegh, 1996; Verhaegh, Duijneveldt, Dhont, & Lekkerkerker, 1996). Small-angle light scattering (SALS) is an obvious choice for studying SD, but as the technique is limited to relatively weakly scattering systems it can not be applied to the milk protein–amylopectin system used in this study.

3. Image analysis

Two different image analysis procedures were used to extract information from the CSLM images. 2-D Fourier transformation was used to determine the characteristic length scale, Λ, in the demixing system. Morphological sieving was used to obtain information on both the domain sizes of the colloid (casein)-rich (Λ_{cr}) and polymer (amylopectin)-rich (Λ_{pr}) areas as well as the characteristic length scale, Λ. Definitions of Λ_{cr}, Λ_{pr} and the characteristic

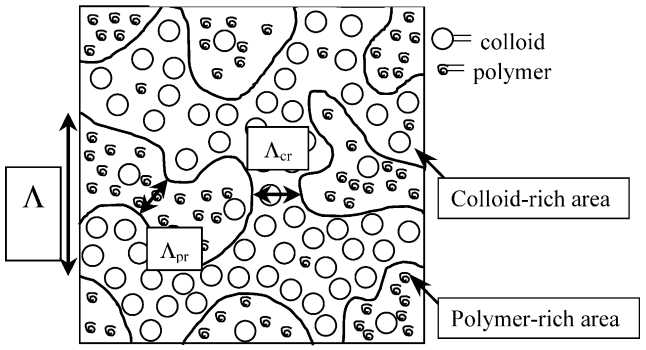

Fig. 1. Sketch of a colloid–polymer system at a certain time during phase separation. The characteristic length scale Λ is defined by $\Lambda = \Lambda_{cr} + \Lambda_{pr}$, with Λ_{cr} is the colloid (casein)-rich domain size and Λ_{pr} is the polymer (amylopectin)-rich domain size.

length scale Λ are given in Fig. 1. Both procedures were implemented using MATLAB (The MathWorks, Inc., USA) and DIPimage (DIPlib, Delft University of Technology, The Netherlands).

3.1. 2-D Fourier transform

2-D Fourier transformation has become a standard image-processing tool; the reader is referred to (Jaehne, 1997) for a detailed description of the technique. 2-D Fourier transforms of the CSLM images were determined and the corresponding power spectra computed. The power spectra were radially averaged to yield a 1-D plot in frequency space. The appearance of a maximum in the plot indicates the presence of a characteristic length scale in the microstructure of the mixture. The characteristic length scales determined from (2-D) micrographs are comparable with length scales determined from light scattering (Guenoun, Gastaud, Perot, & Beyens, 1987; Koenderink et al., 2003).

For non-phase separating or homogenous samples one would expect the intensity of the Fourier Transform to be zero at all frequencies. However, in the course of the experiments it appeared that the intensity in the low-frequency range of the Fourier transform is not zero. Low-frequency contributions were observed for example for a non-phase separating mixture containing 2.7 wt% casein and 1 wt% amylopectin and for an aqueous solution containing milk protein (no amylopectin). Low frequency contributions in the Fourier Transform were also observed for an aqueous solution of Rhodamine B. We believe that contributions in the low frequency region of the Fourier Transform are not related to a characteristic length scale in the microstructure of these samples, but in fact are instrumental artefacts resulting e.g. from (small) imperfections in the (optical) equipment. The measured Fourier Transforms were corrected by subtracting the low-frequency contributions ('background signal'). The same background correction was applied to all measured Fourier Transforms.

To determine the characteristic length Λ the following function was fitted to the 1-D Fourier spectrum:

$$p(\|f\|) = \left(b\frac{\|f\|}{a}\right)^2 \exp\left(-2\frac{\|f\|}{a}\right) \quad (1)$$

where f is frequency, a is location of the peak maximum and b is a scaling factor. The location of the peak maximum is related to the characterisic length by $\Lambda = \Delta/a$, where Δ is the pixel pitch. The function $p(\|f\|)$ did not fit the Fourier data over the full frequency spectrum equally well but the peak location could be determined for most images.

3.2. Morphological sieving

The morphological sieving method was first proposed by Matheron (1975). It is a standard image-processing tool and has been extensively used for, amongst other applications, the analysis of size distributions. An overview of the various applications has been given by Soille (1999). In this work the morphological sieving method was used to determine both the sizes of the amylopectin-rich and protein-rich areas (Λ_{pr} and Λ_{cr}, Fig. 1) as well as the characteristic length Λ. The method is based on two fundamental filter operations: the maximum and minimum filters. These filters replace the value of the pixel being filtered with respectively the maximum or minimum value of all the pixels within the 'neighbourhood'. The neighbourhood is defined by the size and shape of the filter (in our case spherical). By combining these two filters a whole set of morphological operators can be defined. One of the operators thus defined is the 'closing', which is a minimum filter on the output of a maximum filter. A closing removes local minima in an image without affecting other regions. The size of the minima removed depends on the size of the neighbourhood (i.e. filter size) chosen. A series of closing operations with increasing filter sizes will close larger and larger minima in the image, as illustrated in Fig. 2. Minima or darker areas in an image are usually regarded as background; in our case the dark areas are the amylopectin-rich regions in the microstructure.

Maxima, or areas in the images with a high intensity, are typically described as objects (in our case these are the casein-rich domains). These can be removed using the dual operator of the closing, the opening filter, which is a sequence of a minimum and a maximum filter. By applying an opening filter at a range of increasing scales, objects of increasing size are removed. This is similar to a sieve, hence the name morphological sieve.

The result of an opening or closing filter is again an image. The image only shows objects that are larger than the size of the sieve. Segmentation of the individual objects is not always easy and hence counting the number of objects may pose a problem. The problem can be circumvented by 'weighting' the image (i.e. integrating the grey-values).

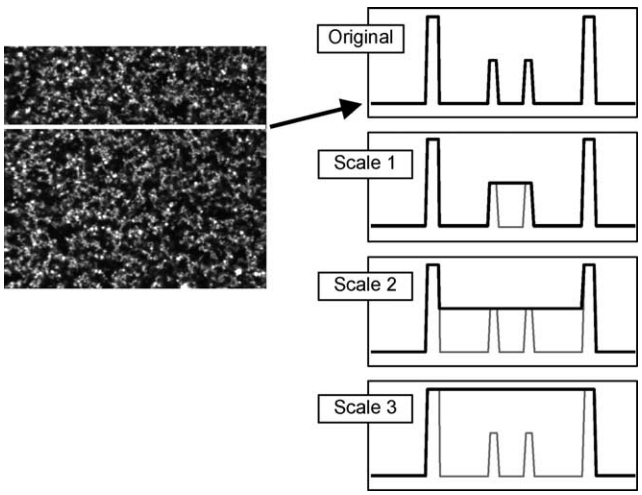

Fig. 2. Schematic explanation of the closing filter. The line labelled 'Original' represents the intensity in the image along the white line. The result of the closing operator on this line at a small size (labelled 'scale 1') is represented by the thick black line superimposed on the original (thin) line. Scales 2 and 3 represent the result of the closing filter at larger scales. Combination of these three scales yields a sieve.

In this way a value is deduced from the image which is related to the number of objects without the need of separating objects. Repeating this procedure for each scale (i.e. filter size) then yields the granulometry (or size distribution). The morphological sieve algorithm as used in this paper is explained in further detail in (Luengo Hendriks, 2004).

The size distribution of the amylopectin-rich (dark) areas has been determined using a closing sieve and that of the protein-rich (bright) areas using an opening sieve. To obtain an estimate of the characteristic length of the structure, we determined the median of the size distribution of each of the phases, and determined the sum ($\Lambda = \Lambda_{pr} + \Lambda_{cr}$). This value was compared to the characteristic size as determined by the Fourier transform method.

The sieving method is very sensitive to isolated peaks in the image (as present in the CSLM images). These cause the size distribution to be biased towards the larger sizes. Therefore, we found it necessary to include a pre-processing step before computing the granulometry. A simple clipping function worked well, but a more complex error-function clip (which introduces less aliasing into the image (van Vliet, 1993)) produced better results. This clipping was tuned to the 99th percentile, i.e. the 1% highest pixel values were clipped.

4. Experimental

4.1. Sample preparation

High-heat skimmed milk powder (e.g. Friesland Coberco Dairy Foods, the Netherlands) was used (water content 2.3 wt%). A concentrated stock solution was prepared by dissolving 28.6 wt% of the powder in demineralised water (overall protein content 10.6% of which 8.5% casein).

Milk-permeate was obtained from a solution of 28.6 wt% of low-heat skimmed milk powder in demineralised H_2O. The solution was ultra-filtrated through a filter with a cut off of 8 nm. The final pH of the permeate was around 6.3. Chemical analysis showed that after filtration 0.6 wt% of proteinaceous material was still present in the permeate. The permeate further contained Ca (0.06%), Mg (0.02%), P (0.1%) and 12.5% of lactose.

The polysaccharide used was an amylopectin extracted from potato starch (ex. AVEBE, the Netherlands). The following characteristics were provided by the supplier: a dry matter content of 964 mg/g, a phosphorus content of 0.78 mg/g (on dry matter) and an amylose content of 0%. A stock solution was prepared by dissolving amylopectin (10 wt%) in milk-permeate at 65 °C under stirring conditions.

All stock solutions were preserved by adding 0.03 wt% of NaN_3. Different mixtures with a casein content of 2.7 wt% and several amylopectin contents (1.0, 1.6, 1,9 and 4.8 wt%) were prepared. This was done by combining appropriate amounts of the milk protein, amylopectin and permeate stock solutions. In this way samples were prepared with similar pH and salt levels. A total amount of 10 g of each sample was prepared. After mixing for $1\frac{1}{2}$ h each sample was transferred to a special sample holder. This sample holder, a glass vessel with a miniature stirrer (Blonk, 2001) could be mounted above the CSLM objective and made it possible to observe the bottom of the sample. After transferring the sample to the glass vessel, stirring was started again. The sample height was approximately 3 cm and measurements were performed at room temperature at a depth of about 5–10 μm from the bottom of the sample.

4.2. Confocal scanning laser microscopy (CSLM)

The proteins were labelled with a solution of Rhodamine B (ex. Aldrich) (0.001 wt%) in demi-water. It was checked that Rhodamine B did not influence the macroscopic phase separation behaviour. Laser light with a wavelength of 568 nm was used to induce fluorescence. Images were made using a Bio-Rad MRC1024 equipped with a Argon/Krypton laser, combined with a Zeiss Axiovert (inverted) microscope. An objective (40 × zoom 2) was used, resulting in an image width of 130 μm, sampled by 512 × 512 pixels. A time series of each sample was recorded. Due to the special sample holder it was possible to record an image just after stirring was stopped. One scan took about 3 s and was Kalman (a noise reduction filter) filtered during creation of the image. The measuring frequency was every 5 or 60 s for 30 or 45 min. The CSLM images gave no indication that sedimentation of protein aggregates played a role during the measurements.

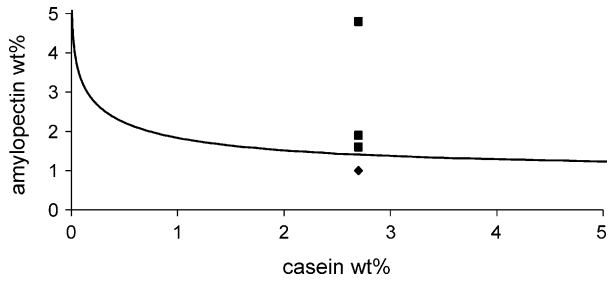

Fig. 3. Phase diagram of casein–amylopectin mixtures (reproduced from de Bont et al., 2002). The mixtures examined in this study are represented by ■ (= phase separating mixture) and ◆ (= non-phase separating mixture). The drawn line represents the phase boundary curve.

5. Results and discussion

The phase separation behaviour of milk protein–amylopectin mixtures at pH 6.3 is described in detail in de Bont et al. (2002). The phase diagram is reproduced in Fig. 3. The figure also shows the composition of the various mixtures used in this study. All mixtures had a constant casein content (2.7 wt%) and were located on a vertical cross-section through the phase diagram. The mixture containing 1.0% amylopectin is a non-phase separating system. Those containing 1.6% and 1.9% amylopectin are close to the phase boundary, whereas the one with the largest amount of amylopectin (4.8%) lies far in the region where phase separation occurs.

5.1. Microscopic observations (CSLM)

CSLM images of the various mixtures measured after 0, 10, 20 and 30 min are presented in Fig. 4. The images obtained at 0 min are representative for a non-phase separated system (although some details can be seen in the micrographs). The image of the 1.0% amylopectin/2.7% casein mixture does not change over time; the other mixtures clearly show phase separation, with protein-rich areas (white) and amylopectin-rich areas (black) developing over time. The protein-rich areas appear to form aggregate-like structures. Qualitatively, the appearance of the protein-rich areas is similar to that of rennet- or acid-induced milk protein aggregates. The size of the protein-rich areas (at a certain point in time) depends on the amount of amylopectin present in the mixture and decreases with increasing amylopectin concentration. At low amylopectin

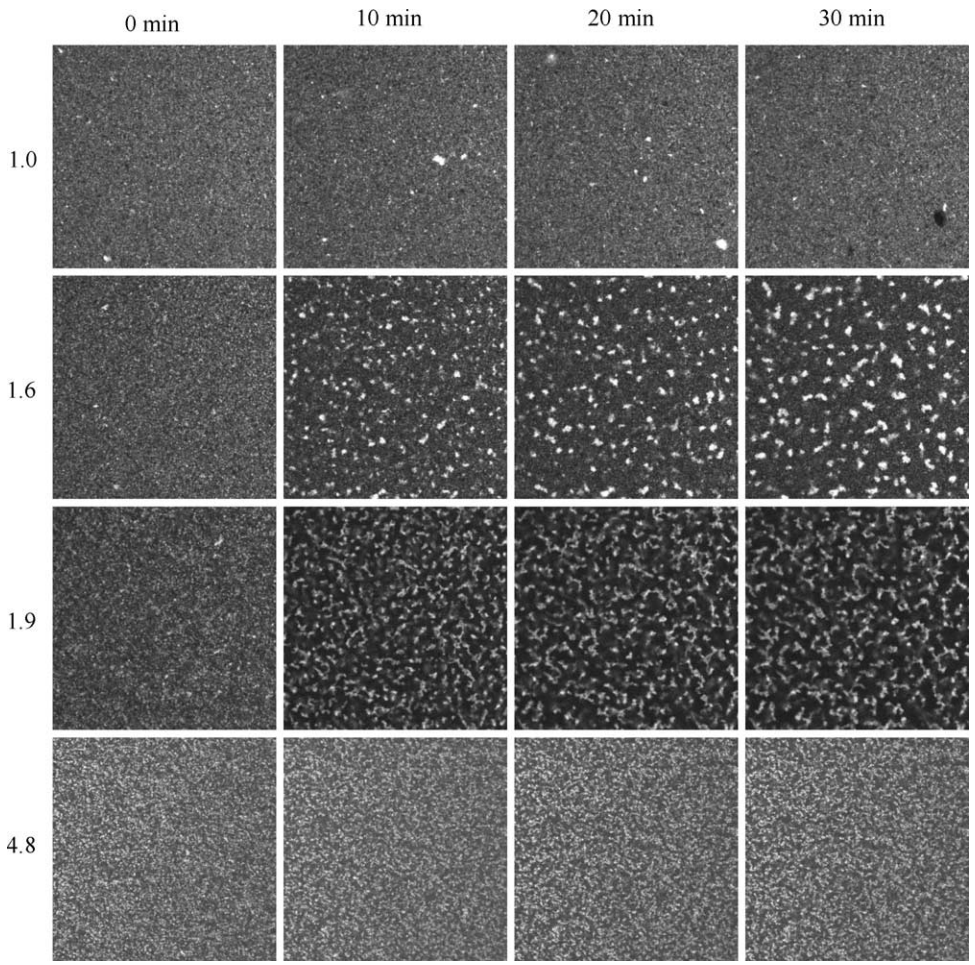

Fig. 4. CSLM images of milk protein–amylopectin mixtures. All mixtures contain 2.7 wt% casein and 1.0, 1.6, 1.9 or 4.8% amylopectin (from top to bottom). The images were made at 0, 10, 20 and 30 min after stirring was stopped (from left to right). Image width: 130 μm.

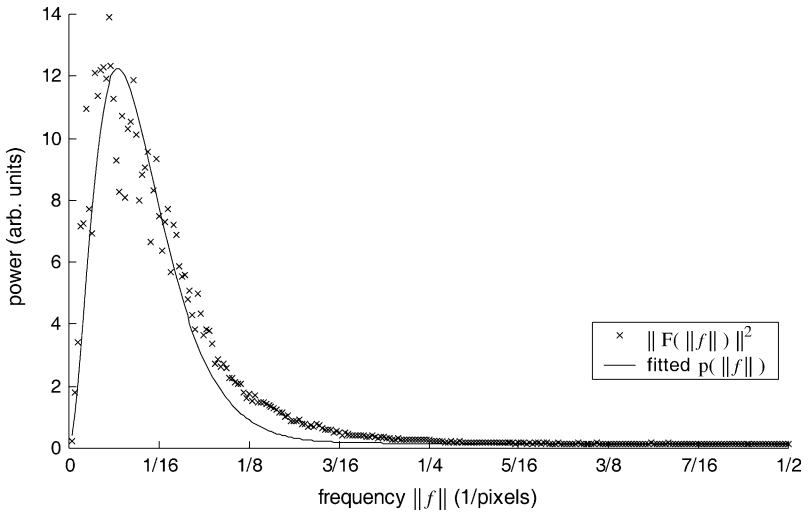

Fig. 5. Radially averaged frequency spectrum of one of the CSLM images (4.8 wt% amylopectin, $t = 30$ min) shown in Fig. 4. The drawn line represents a best fit as explained in the text.

concentrations the protein aggregates appear to be more isolated, whereas at higher concentration they are more connected. A scan in the z-direction (i.e. perpendicular to the horizontal plane of observation) from the bottom of the sample up to 40 μm revealed that the protein-rich areas are indeed interconnected (i.e. form a 3-D network) at the highest (4.8 wt%) amylopectin concentration. The CSLM images do not allow us to distinguish between SD and NG. It is noted that the size of the protein- and amylopectin-rich areas in the mixtures containing 1.6 and 1.9 wt% amylopectin becomes comparable to the distance from the wall of the sample cell at which the CSLM picture were taken (5–10 μm). We can not exclude that wall effects to some extent have influenced the growth of the areas.

5.2. Image analysis: 2-D Fourier transform (FT)

Fig. 5 shows an example of a radially averaged frequency spectrum. The appearance of a maximum in the plot clearly indicates the presence of a characteristic length scale in the microstructure. The variation of the characteristic length scale with time is shown in Fig. 6 for the various mixtures studied. All growth curves show a power-law time dependence. The exponents observed for the mixtures containing 1.6 and 1.9 wt% amylopectin are $\alpha = 0.23$ and $\alpha = 0.21$, respectively. These values are typical for demixing mixtures in the later stages of NG or SD. The sample containing 4.8 wt% amylopectin also shows power law behaviour, but the exponent is much lower in this case: $\alpha = 0.04$. The low value of α is tentatively attributed to the formation of a protein aggregate network in this system with gel-like properties (de Bont et al., 2002). Gelation is expected to slow down coarsening of the microstructure as it hinders diffusion and reduces mobility of the components in the mixture. The coarsening exponent α is therefore lower than the values observed in non-gelling mixtures. Low values of α have been predicted for late stage coarsening in mixtures where gelation occurs (Onuki et al., 1999) and have been reported in experimental studies on a.o. gelling gelatin/maltodextrin systems (Butler, 2002) and xanthan–colloid mixtures at relatively high xanthan concentrations (Koenderink et al., 2003).

A characteristic feature of SD is a constant characteristic length scale in the initial stage of demixing. From the results in Fig. 6 it is clear that the characteristic length scale in the amylopectin–milk protein system increases directly from the onset of the measurements. This, however, does not imply that demixing in the amylopectin–milk protein system does not occur through SD. It is conceivable that demixing occurs via SD, but that the initial stage of decomposition is outside our experimental window (i.e. the initial phase is too short).

Fig. 7 shows the variation of the peak height, I_{max}, with time. Power-law growth is observed for all

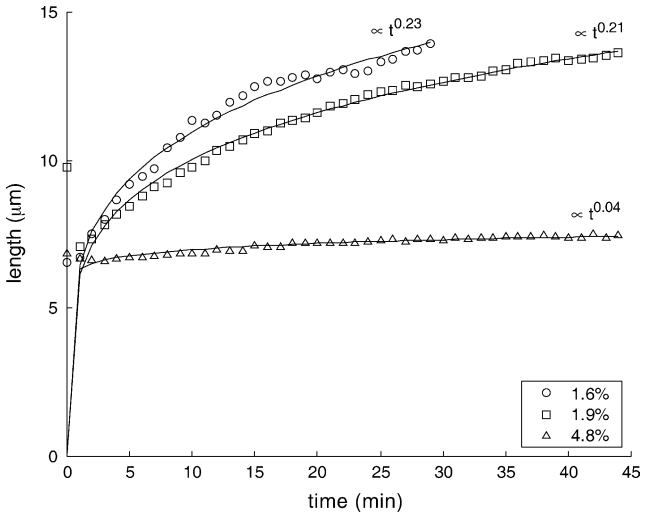

Fig. 6. Characteristic length scale as a function of time as determined with the Fourier transform method. Mixtures contain 2.7 wt% casein and 1.6, 1.9 and 4.8 wt% amylopectin, respectively.

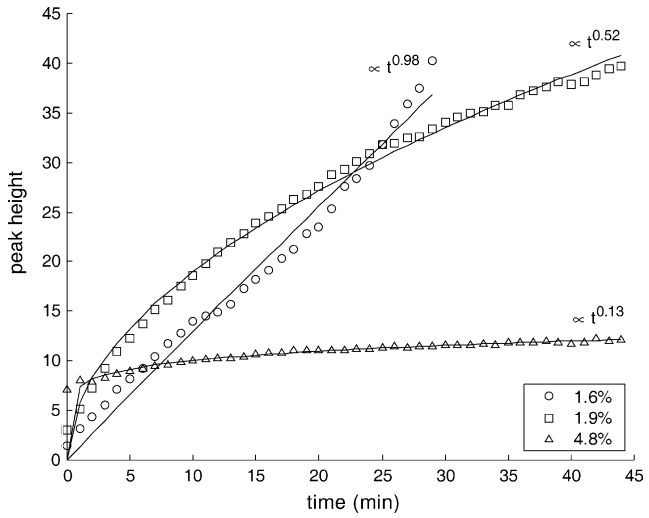

Fig. 7. Maximum intensity in the Fourier spectrum as a function of time. The mixtures contain 2.7 wt% casein and 1.6, 1.9 and 4.8 wt% amylopectin, respectively.

amylopectin–milk protein mixtures studied, $I_{max} \propto t^{\beta}$. The growth exponents are $\beta = 0.98$, 0.52 and 0.13 for mixtures containing 1.6, 1.9 and 4.8 wt% amylopectin, respectively. Theories for SD predict $\beta/\alpha = 3$ in both the early and late stages of demixing (Binder and Stauffer, 1974; Hashimoto, Itakura, & Hasegawa, 1986; Siggia, 1979). The following ratio's are calculated: $\beta/\alpha = 4.3$, 2.5 and 3.3 for mixtures containing 1.6, 1.9 and 4.8 wt% amylopectin, respectively. These values seem compatible with theoretical predictions.

5.3. Image analysis: morphological sieving (MS)

Growth curves obtained by applying the morphological sieving (MS) method are shown in Fig. 8. As explained in paragraph 3.2 the CSLM images were pre-processed before applying the MS-method. The curves show power-law behaviour with exponents of 0.22, 0.16 and 0.03 for samples containing 1.6, 1.9 and 4.8 wt% amylopectin, respectively. The growth exponents are very similar to the values determined by the Fourier transform method. The characteristic length scales determined by the two methods are also in good agreement, except for the mixture containing 4.8 wt% amylopectin. In the latter case the values determined by the MS method are lower than those obtained by the Fourier transform method. The reason for this difference is not clear.

Fig. 9 shows the growth of the (median) casein- and amylopectin-rich domain size. Information on the individual domain sizes can not be obtained via the Fourier transform method. Power-law growth is observed for both domains. However, different power-law exponents are observed for the different domains, with the amylopectin-rich domains growing faster (i.e. larger α)

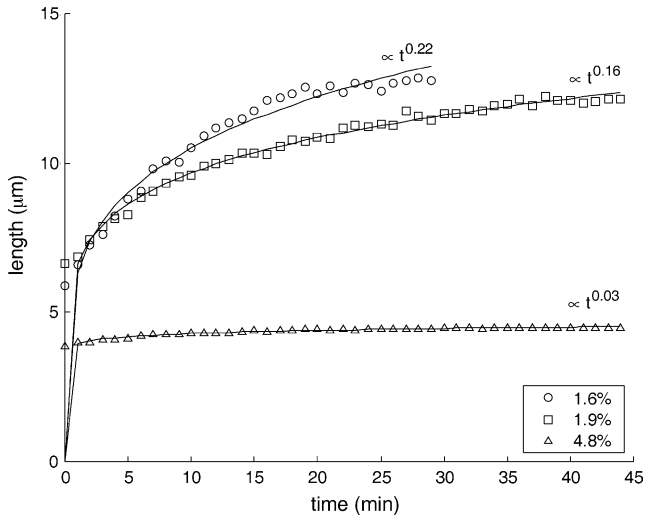

Fig. 8. Characteristic length scale (= median size of casein-rich domains plus median size of amylopectin-rich domains) as a function of time determined with the morphological sieving method. Mixtures contain 2.7 wt% casein and 1.6, 1.9 and 4.8 wt% amylopectin, respectively.

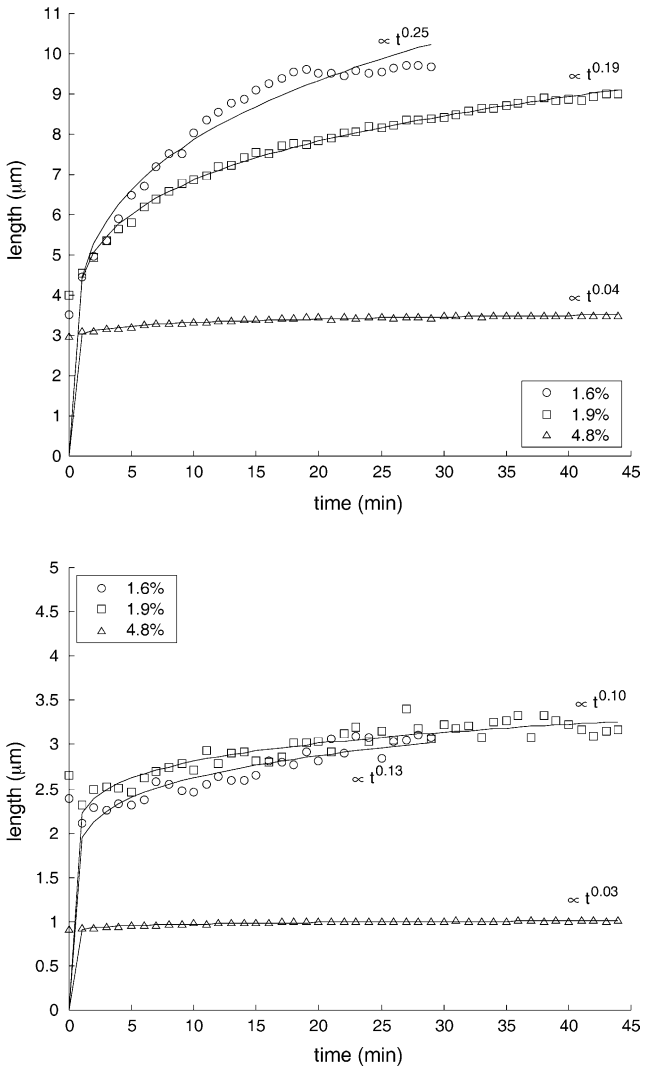

Fig. 9. Median size of amylopectin-rich (top) and casein-rich domains (bottom) as a function of time as measured with the morphological sieving method. The mixtures contain 2.7 wt% casein and 1.6, 1.9 and 4.8 wt% amylopectin, respectively.

than the casein-rich domains. This result is rather unexpected in view of the generally accepted idea that the domain pattern is self-similar in time in the late stage of phase separation. The self-similarity concept implies that the morphology of the system is characterised by only one length scale and one would therefore expect the casein- and amylopectin-rich domains to grow with similar power-law kinetics. Not all systems show self-similar domain growth in the late stage of phase separation, however (Tanaka, 2000). At this stage it is not clear whether our results indicate a deviation from self-similarity or whether the different growth behaviour of the casein- and amylopectin-rich domains is related to the morphological sieving procedure used (e.g. choice of filter shape). This will be studied in further detail.

6. Conclusion

The time evolution of phase separating milk protein—amylopectin mixtures at pH 6.3 was studied by CSLM. The CSLM images were analysed using different methods. The Fourier transform method revealed the existence of a characteristic length scale in the system, which evolved with time according to a power law, $\Lambda \sim t^{\alpha}$. The observed exponents are $\alpha = 0.23$ and 0.21, for mixtures containing 1.6 and 1.9 wt% amylopectin, respectively. These values are typical for demixing mixtures in the later stages of NG or SD. For a mixture containing 4.8 wt% amylopectin the observed power is ca. 0.04; a low value of α has been predicted by coarsening theory in mixtures of gelling (bio-) polymers. Growth curves obtained by the Fourier transform method agree well with those obtained using the morphological sieving method, adding additional confidence to the obtained results. The sieving method yielded different values of α for casein- and amylopectin rich domains; the origin of this difference is not clear yet.

Acknowledgements

AVEBE is kindly acknowledged for supplying the potato amylopectin and Friesland Coberco Dairy Foods for supplying the high heat skimmed milk powder. Special thanks to Cees Vooys of Unilever Research and Development Vlaardingen for his useful assistance during the CSLM measurements. Liesbeth de Jong, Igor Bodnar and Rob Groot are kindly acknowledged for fruitful discussions. This study was supported by the PBTS Research Program with financial aid from the Ministry of Economical Affairs and by the Integral Structure Plan for the Northern Netherlands from the Dutch Development Company.

References

Binder, K., & Stauffer, D. (1974). Theory for slowing down of relaxation and spinodal decomposition of binary-mixtures. *Physics Review Letters*, *33*, 1006–1009.

Blonk, J. C. G (2001). Viewing Food Microstructure. *Eighth International Congress on Engineering and Food, 9–13th April 2000, Mexico*.

de Bont, P. W., van Kempen, G. M. P., & Vreeker, R. (2002). Phase separation in milk protein and amylopectin systems. *Food Hydrocolloids*, *16*, 127–138.

Bourriot, S., Garnier, C., & Doublier, J-L. (1999a). Phase separation, rheology and microstructure of micellar casein–guar gum mixtures. *Food Hydrocolloids*, *13*(1), 43–49.

Bourriot, S., Garnier, C., & Doublier, J-L. (1999b). Phase separation, rheology and structure of micellar casein–galactomannan mixtures. *International Dairy Journal*, *9*(3/6), 353–357.

Bourriot, S., Garnier, C., & Doublier, J-L. (1999c). Micellar casein-(-carrageenan mixtures. I. Phase separation and ultrastructure. *Carbohydrate Polymers*, *40*(2), 145–157.

Butler, M. F., & Heppenstall-Butler, M. (2001). Phase separation in gelatin/maltodextrin and gelatin/maltodextrin/gum arabic mixtures studied using small-angle light scattering, turbidity and microscopy. *Biomacromolecules*, *2*(3), 812–823.

Butler, M. F. (2002). Mechanism and kinetics of phase separation in a gelatin/maltodextrin mixture studied by small-angle light scattering. *Biomacromolecules*, *3*(4), 676–683.

Cahn, J. W., & Hilliard, J. E. J. (1958). *Chemistry Physics*, *92*, 258.

Cahn, J. W. (1965). Phase separation by spinodal decomposition in isotropic systems. *Journal Chemistry Physics*, *42*, 93.

de Kruif, C. G. (1992). Casein micelles: diffusivity as a function of renneting time. *Langmuir*, *8*(12), 2932–2937.

DIPlib: The Delft Image Processing Library, http://www.ph.tn.tudelft.nl/DIPlib, Pattern Recognition Group, TU-Delft, the Netherlands.

Dhont, J. K. G. (1996). *An Introduction to Dynamics of Colloids*. Amsterdam: Elsevier Science.

Guenoun, P., Gastaud, R., Perrot, F., & Beyens, D. (1987). Spinoal decompositionpatterns in an isodensity critical binary fluid—Direct visualization and light scattering analysis. *Physics Review A*, *36*, 4876–4890.

Hashimoto, T., Itakura, M., & Hasegawa, H. (1986). Late stage spinodal decomposition of a binary polymer mixture. 1. Critical test of dynamic scaling in scattering function. *Journal Chemistry Physics*, *85*, 6118–6128.

Jaehne, B. (1997). *Practical Handbook on Image Processing for Scientific Applications*. Bocaraton, FL: CRC Press.

Koenderink, G. H., Aarts, D. G. A. L., de Villeneuve, V. W. A., Philipse, R., Tuinier, R., & Lekkerkerker, H. N. W. (2003). Morphology and kinetics of phase separating transparant xanthan–colloid mixtures. *Biomacromolecules*, *4*, 129–136.

Lekkerkerker, H. N. W., Poon, W. C. K., Pusey, P. N., Stroobants, A., & Warren, P. B. (1992). Phase behaviour of colloid + polymer mixtures. *Europhysics Letters*, *20*(6), 559–564.

Lifshitz, I. M., & Slyozov, V. V. (1961). The kinetics of precipitation from super-saturated solid solutions. *Journal Physics Chemistry Solids*, *19*, 35–50.

Lorén, N., Altskär, A., & Hermansson, A. M. (2001). Structure evolution during gelation at later stages of spinodal decomposition in gelatin/maltodextrin mixtures. *Macromolecules*, *34*, 8117–8128.

Lorén, N., Langton, M., & Hermansson, A. M. (2002). Determination of temperature dependent structure evolution by fast-Fourier transform at late stage spinodal decomposition in bicontinuous biopolymer mixtures. *Journal Chemistry Physics*, *116*, 10536–10546.

Luengo Hendriks, C. L (2004). *Structure Characterisation using Mathematical Morphology*. PhD Thesis, Delft University of Technology, The Netherlands.

Matheron, G. (1975). *Random Sets and Integral Geometry*. New York: Wiley.

Onuki, A., & Puri, S. (1999). Spinodal Decomposition in Gels. *Physical Review E*, *59*, R1331–R1334.

Rouw, P. W., Woutersen, A. T. J. M., Ackerson, B. J., & de Kruif, C. G. (1989). Adhesive hard sphere dispersions. *Physica A*, *156*, 876–898.

Schorsch, C., Clark, A. H., Jones, M. G., & Norton, I. T. (1999). Behavior of milk protein/polysaccharide systems in high sucrose. *Colloids and Surfaces B*, *12*(3-6), 317–329.

Schorsch, C., Jones, M. G., & Norton, I. T. (1999). Thermodynamic incompatibility and microstructure of milk protein/locust bean gum/sucrose systems. *Food Hydrocolloids*, *13*(2), 89–99.

Siggia, E. D. (1979). Late stages of spinodal decomposition in binary-mixtures. *Physics Review A*, *20*(2), 595–605.

Soille, P. (1999). *Morphological Image Analysis*. Berlin: Springer.

Sperry, P. R. (1984). Morphology and mechanism in latex flocculated by volume restriction. *Journal of Colloid and Interface Science*, *99*(1), 97–108.

Tanaka, H. (2000). Viscoelastic Phase Separation. *Journal of Physics D: Condensed Matter*, *12*, 207.

Tokuyama, M., & Kawasaki, K. (1984). Statistical–mechanical theory of coarsening of spherical droplets. *Physica A*, *123*, 386.

Tromp, R. H., Rennie, A. R., & Jones, R. A. L. (1995). Kinetics of the simultaneous phase separation and gelation in solutions of dextran gelatin. *Macromolecules*, *28*, 4129–4138.

Tuinier, R. (1998). Depletion flocculation of casein micelles induced by the EPS of a lactic acid bacterium. In C. G. de Kruif (Ed.), (*vol. 9*) (pp. 222–230). *Gums and Stabilisers for the Food Industry*, Cambridge: Royal Society of Chemistry.

Tuinier, R., & de Kruif, C. G. (1999). Phase behaviour of casein micelles/exocellular polysaccharide mixtures: experiment and theory. *Journal of Chemical Physics*, *110*(18), 9296–9304.

Tuinier, R., Dhont, J. K. G., & de Kruif, C. G. (2000). Depletion-induced phase separation of aggregated whey protein colloids by an exocellular polysaccharide. *Langmuir*, *16*(4), 1497–1507.

Verhaegh, N. A. M (1996). *Structure and kinetics of phase separating colloidal suspensions*. PhD Thesis, ISBN 90-393-1327-X, The Netherlands.

Verhaegh, N. A. M., Duijneveldt, J. S., Dhont, J. K. G., & Lekkerkerker, H. N. M. (1996). Fluid–fluid phase separation in colloid–polymer mixtures studied with small angle light scattering and light microp-scopy. *Physica A*, *230*, 409–436.

van Vliet, L. J (1993). *Grey-scale measurements in multi-dimensional digitized images*. PhD Thesis, Pattern Recognition Group, Faculty of Applied Physics, Delft University of Technology, Delft.

Vrij, A. (1976). Polymers at interfaces and the interactions in colloidal dispersions. *Pure and Applied Chemistry*, *48*(4), 471–483.